

Self-Calibrating Scalable Research Platform for Ultrasonic Measurements in Chemical and Biological Reactors

A. N. Kalashnikov¹, V.G. Ivchenko¹, R. E. Challis¹, W. Chen¹

¹School of Electrical and Electronic Engineering, University of Nottingham, University Park, Nottingham, NG7 2RD, UK

Abstract – A research platform that integrates high accuracy FPGA waveform acquisition architectures and MATLAB graphical user interface is described. The platform provides self-calibrating measurements and frame jitter free operation. The FPGA architectures were tested on two different chips using the same user interface successfully. Examples of the platform utilization for monitoring of chemical and biological reactors are presented.

Keywords – ultrasonic NDE instrumentation, monitoring of chemical and biological processes, self-calibrating measurements

I. INTRODUCTION

Ultrasonic NDE instrumentation involves formation of the excitation signal, its delivery to a piezoelectric transducer for radiation, amplification of the received echo or transmitted through the inspection object response, its digitization, preliminary and secondary digital signal processing. The interrogation results are presented to the end user as A-scans (ultrasonic NDE) or C-scans (medical ultrasound) by off-the-shelf commercial equipment. Effective research of new applications of the ultrasonic inspection techniques requires access to raw high accuracy ultrasonic records [1]. Recent special issue of IEEE Transactions on UFFC addressed this need by presenting six papers devoted to description of various research platforms that provide clinicians with an access to raw ultrasonic data [2]. However availability of such platforms also seems essential for ultrasonic NDE because different processing methods are applicable to extract information from the raw records (e.g., [3]). Operators that allow an ultrasonic NDE researcher to concentrate on the validity of experimental conditions and on information extraction seem rarely available off the shelf, as medical ultrasound systems include some operations redundant for mainstream ultrasonic NDE like beamforming [2]. NDE platforms available commercially (e.g., [4]) lack a self-calibration feature that is central for reliable measurements.

A typical ultrasonic measurement system contains four distinct parts, shown in the table. They could all come from different suppliers, and modularity of the system allow for upgradeability. Until recently the less flexible part was the digital one because of the hardwired design approach that was only possible at frequencies of interest. FPGA technology enabled continuous development based on some existing hardware by reconfiguring it, and porting of an existing design into some newer hardware. Contemporary applications of ultrasonic instruments move towards higher

spatial resolution (higher operating frequencies), higher attenuation media and weaker contrast (lower signal to noise ratio).

Therefore the principal considerations that steered our developments were as follows: use of easily reconfigurable and programmable FPGA development board, achieving high accuracy of ultrasonic data acquisition through provisions of high sampling frequencies and extensive averaging, ensuring scalability and self-calibrating features, and providing a convenient user interface to the instrument control and measured data. This research was funded by the EPSRC (UK).

The table. Structure of a typical single channel ultrasonic instrument

	Transducer	Analogue	Digital	PC
Receiver	0.5-30 MHz typical	Amplifier (signal conditioning)	Digitisation and preliminary processing (averaging, matched and spectral filtering)	Secondary processing (spectral calculations, parameter estimation)
Transmitter	The same as above	Transducer driver (2 nF load)	Waveform generator (digitised samples plus DAC or binary code)	Trigger

II. UNCERTAINTY IN ULTRASONIC MEASUREMENTS AND PROVISIONS FOR ITS REDUCTION IN THE PLATFORM

Any ultrasonic instrument extracts information from digitized time-domain records, for example, attenuation and velocity spectra [5] or parameters of particular models [6]. Inaccuracies in the records lead to uncertainty in the end result, and these inaccuracies are frequently magnified because the extraction process contains non-linearities [5, 6]. Although the uncertainty magnification depends on measurement conditions, an instrument that records signals with higher accuracy will deliver lower uncertainty at the same conditions. Fig.1 shows inaccuracies associated with recording of a ramp signal (black solid line, ideal samples shown by crosses). Additive noise distorts the waveform as it is shown by the blue line. Ideally sampling will result in samples shown in fig.1b. However presence of some clock oscillator instability, and aperture jitter of the ADC result in sampling at slightly different times (fig.1c, timing jitter). Finally, the samples are quantized giving output codes that might contain substantial errors (fig.1d).

Decreasing the influence of the above errors requires appropriate design of the instrument itself, its operating

conditions and signal processing procedures applied [5]. First of all the sampling frequency should be high enough (ten or more times the transducer's centre frequency is employed routinely). The operating frequency of the digital part around 500 MHz is thus required for a 50 MHz transducer. That imposes significant cost of the ADC, and difficulties in digital design as most high-level design toolboxes for CAD packages limit operating frequencies far below the ultimate capabilities of an FPGA IC itself. We employed interleaving to address the need for the high sampling frequency [7, 8].

Reduction of the additive noise was provided by the use of averaging [9]. Averaging can bring some inaccuracies if the subsequent records are not coherent fully because of the frame jitter [10]. The latter can be reduced by synchronizing the transmitter and receiver digital parts (the table). Such synchronization is also essential for the correct operation of the interleaved sampling.

These two approaches were combined and implemented using a commercially available FPGA development board [11]. Subsequent developments included extensions to its initial capabilities including elaborated user interface that controls acquisition of two independent sections of the input waveform. This allows self-calibration of the instrument based on a single record as shown below, which reduces uncertainty related to non-identity of measurement conditions between the calibration and measurement records.

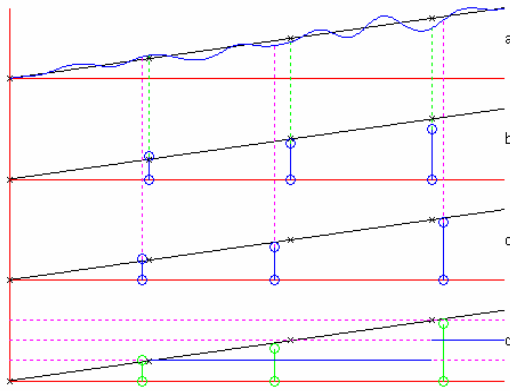


Fig.1. Inaccuracies that affect digitizing of a ramp signal (solid black line, ideal samples shown by the crosses; a – ideal and noisy continuous waveforms, b – sampled noisy waveform, c – noisy waveform sampled with timing jitter, d – quantized sampled with timing jitter noisy waveform)

III. USING THE PLATFORM FOR ULTRASONIC MEASUREMENTS IN A CHEMICAL REACTOR

The platform was applied for monitoring of chemical reactions using operators and procedures reported previously

[3]. The graphical user interface (fig.2) allows the user to select two windows for data acquisition independently. One of these is reserved for capturing the excitation pulse that is required because ultrasonic pulsers that excite transducers introduce variable delay to the input pulses as a result of environmental influence on pulser's operation. The second window is used for capturing the response of the interrogated medium (fig.3). The time difference between the two

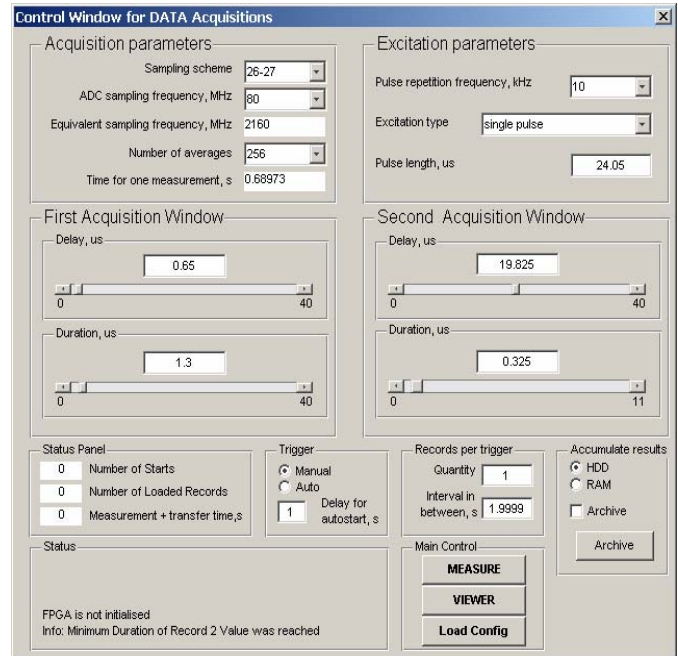


Fig.2. Screenshot of a graphical user interface developed in MATLAB

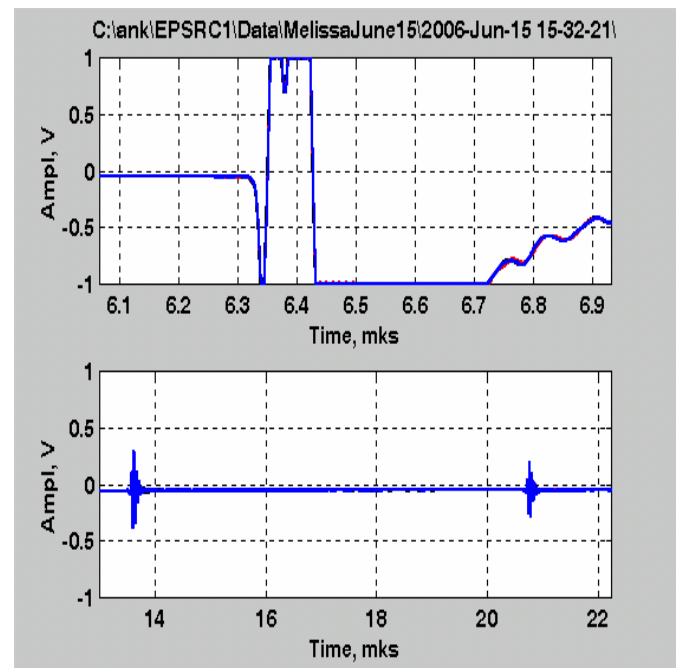


Fig.3. Use of two acquisition windows to capture both the excitation pulse and the response

waveforms informs on the state of the medium, and elimination of the warming up influence allows monitoring with an accuracy improved by up to 10% in some experiments.

Titration curves obtained for two sets of experiments are presented in fig.4-5. The black lines show measured time delays of the ultrasonic pulse in μs versus the experiment time in seconds (each drop was applied in 30 seconds interval). The red line shows how these delays were compensated for temperature as described in [12].

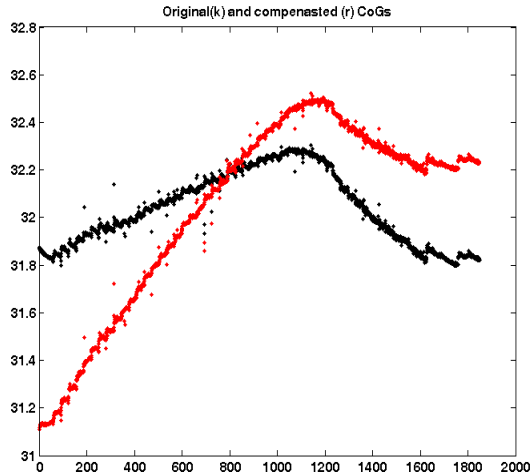


Fig.4. AlCl_3 (weak acid) and NH_4OH (weak base, 50 drops of about 200 ppm each) titration. The curve shows a distinct equilibrium point.

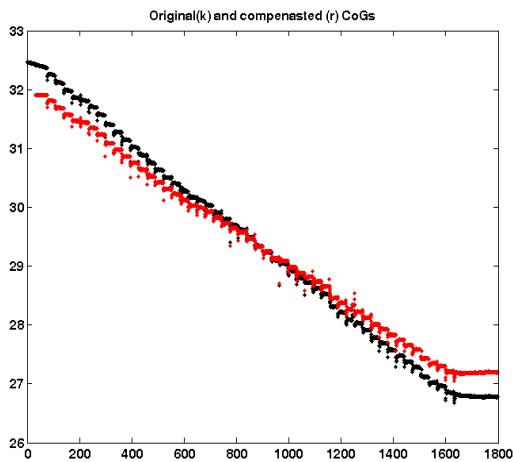


Fig.5. AlCl_3 (weak acid) and Na_2SO_4 (weak base, 50 drops of about 440 ppm each) titration. The curve does not show much of an interaction.

IV. USING THE PLATFORM FOR ULTRASONIC MEASUREMENTS IN A BIOLOGICAL REACTOR

Another application relates to production of bio-materials in high pressure bioreactors that were found difficult to monitor by optical techniques. The fabrication process involved several phase transitions of the raw powder into a final air-bubbled bio-material through a liquid phase. Measuring the reflection coefficient of the evolving medium contacting a sapphire window monitored these transitions in our initial experiments. The measurements required high accuracy as the anticipated change in the reflection coefficient was rather small, and self-calibration was found essential as the acoustic contact between the window and the transducer pressed against it varied with variation of pressure in the reactor (fig.6). Fig.7 shows the improvement in the curves when the reflection coefficient was self-calibrated by using the ultrasonic triple transit signal.

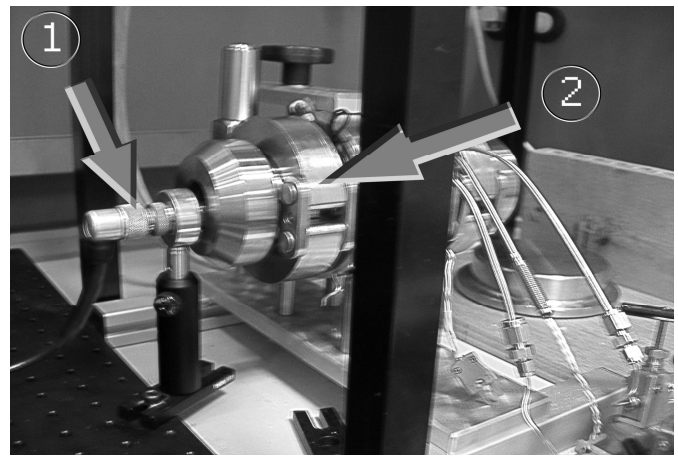


Fig.6. Experimental setup for ultrasonic monitoring of a high pressure biological reactor; 1 - ultrasonic transducer, 2 - biological reactor

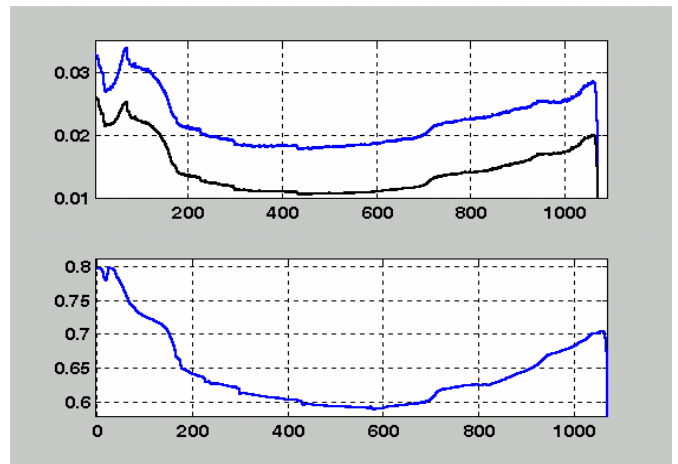


Fig.7. Scattered measured amplitudes of the single transit and triple transit signals (above), and smoother deduced reflection coefficient versus a number of a record acquired

V. IMPROVEMENTS TO THE WAVEFORM GENERATION ALLOWING LOW VOLTAGE OPERATION

In the experiments reported above a pulse excitation was used. The trigger pulse was formed by the FPGA IC, and sent to the external analogue front end unit (Ultrasonic Pulser-Receiver [13]). The latter unit generated high voltage up to 100 V with the binary excitation pulse of a programmable duration. Although some frame jitter increase was observed in the signal pathway, its overall level remained negligibly low. However operation using high voltage could be hazardous in some industrial conditions. Therefore low voltage operation is mandatory for some applications, and it results in dramatic decrease in the signal-to-noise ratio. Use of coded excitation allows compensating for that. This capability was implemented in the platform by using reconfigurable memory inside the FPGA that held up to 8192 samples of the required output signal, 16 bits each. When triggered, the memory outputs these samples to the on-board DAC at a sampling rate of 80 MHz for the examples below. The availability of the on board DAC does not restrict the output values to be binary only; but this mode (that requires the least memory per sample and no DAC at all for a custom instrument) was tested as well.

A. Excitation of chirp waveforms

Chirp waveforms could deliver substantial energy over their duration, but be compressed back into a much shorter wave packet by matched filtering [14]. The efficiency of the chirp excitation increases with the increase of the pulse width and the frequency deviation; however, limited bandwidth of any ultrasonic transducer will limit the effect. Fig. 8 shows experimental results obtained for an ultrasonic transducer with the central frequency of 10 MHz and 40% relative bandwidth that was used for all the experiments with low voltage excitation. It shows two options for the chirp waveform duration (140 and 280 samples, these lengths were chosen to end the waveform by a zero amplitude sample), and two options for the deviation (8..12 MHz and 9..11 MHz ranges). The upper graphs show the samples generated (crosses), joined by the solid line. The middle graphs present the autocorrelation function (ACF) of the chirp calculated out of these samples (crosses, again joined by the solid line). The bottom graphs exhibit the experimental cross-correlation function (CCF) between the received signal and the excitation samples. The best match between the experimental and theoretical responses was observed for the longer pulse with the smaller deviation (fig.8). The processed signal contains numerous side lobes that might be lowered by other means of coded excitation.

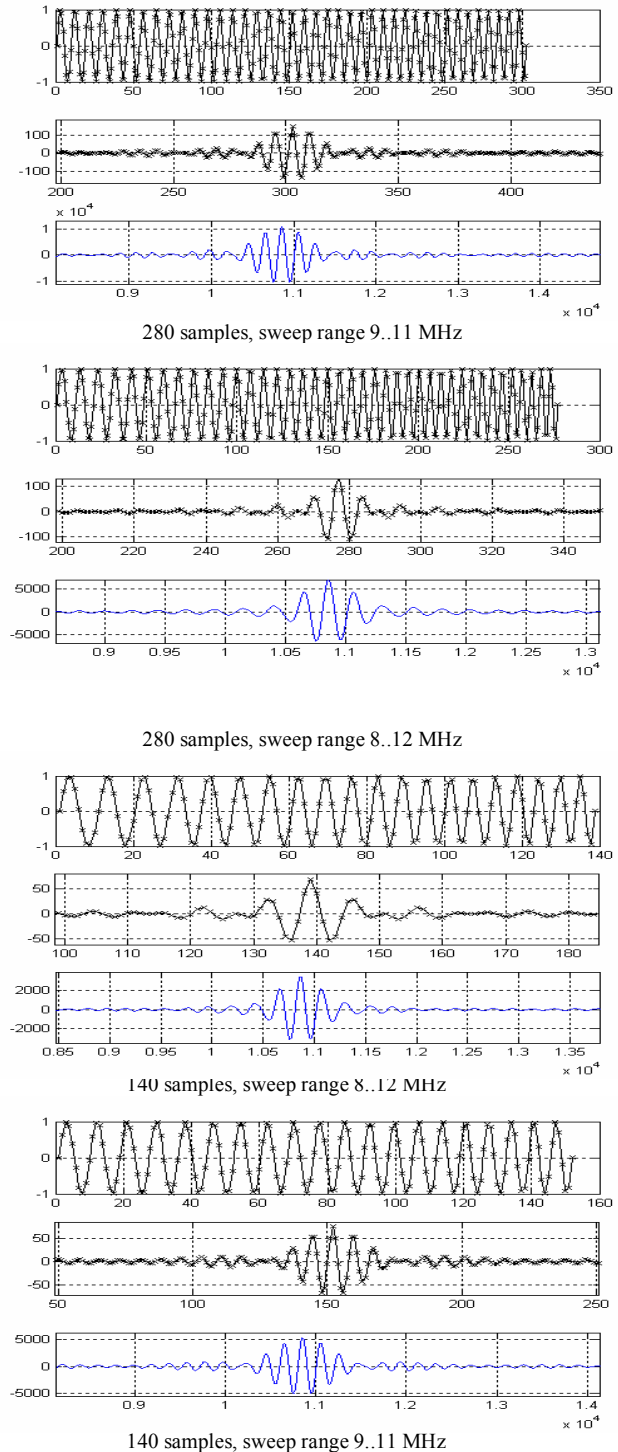
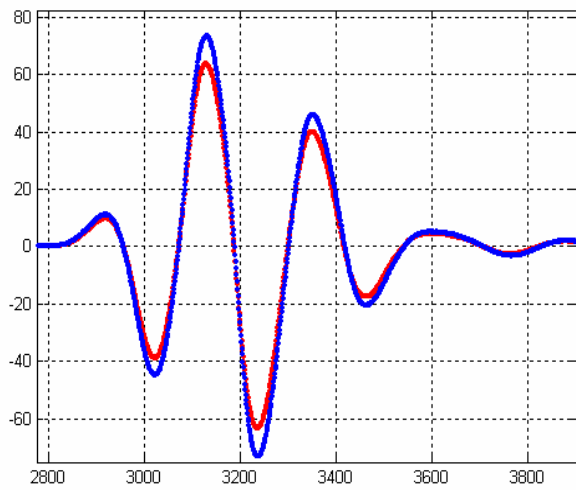


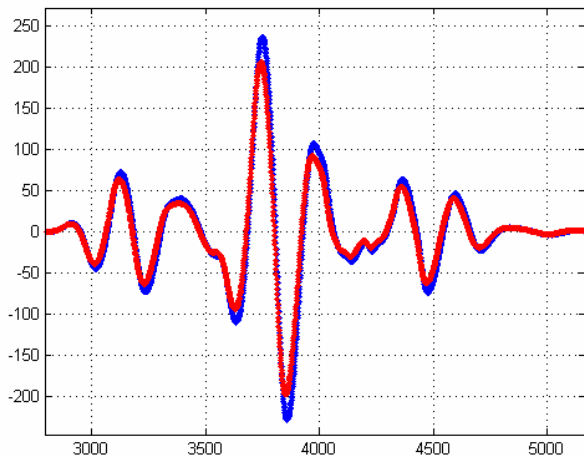
Fig.8. Experiments with the chirp excitation with different waveform durations and frequency deviations

B. The Barker code

This code involves manipulation of the phase of pulses in the excitation packet [15]. The pulse itself can be formed differently by the DAC, and several options were tested. Fig. 9a shows the received waveforms for a single pulse, excited by sequences $[0 \ 0.707 \ 1 \ 0.707 \ 0 \ -0.707 \ -1 \ -0.707]$ and $[0 \ 1 \ 1 \ 1 \ 0 \ -1 \ -1 \ -1]$ that are very similar to each other. The same applies to the waveforms that were recorded for a Barker code of the length 4 (fig.9b). Moreover, when the excitation pulse itself was coded in binary $[01110000]$, the CCF of the received signal resembles the theoretical one for all the known Barker codes (fig.10 presents the experimental CCF for the length of 13).



a



b

Fig.9. Experimental responses to excitation sequences of $[0 \ 0.707 \ 1 \ 0.707 \ 0 \ -0.707 \ -1 \ -0.707]$ (red line) and $[0 \ 1 \ 1 \ 1 \ 0 \ -1 \ -1 \ -1]$ (blue line)
 a – single excitation sequence
 b – excitation sequences arranged in a Barker code of length 4

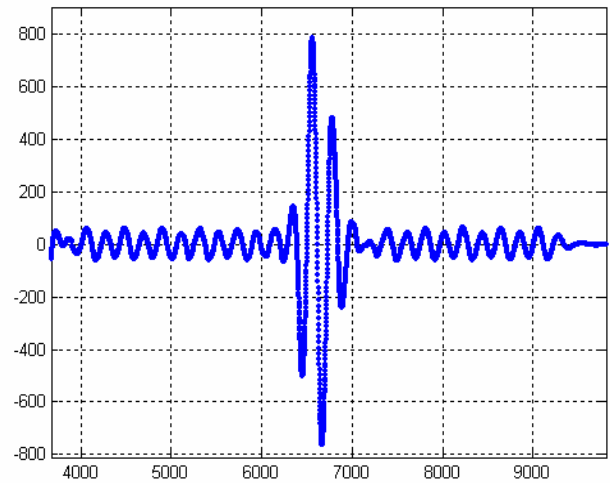


Fig.10. Experimental CCF for the Barker code of length 13

C. Maximum length sequences

Like the Barker codes, these sequences employ phase manipulation of pulses in the excitation packet [16]. However they have higher side lobes of their ACFs than the Barker codes, and the experimental CCF (fig.13) confirms their inferiority in this respect. On the positive side, they can have significant length (fig.11 shows the CCF for the code length of 31), and use 3 or 5 distinct signal levels (thus a simple ADC).

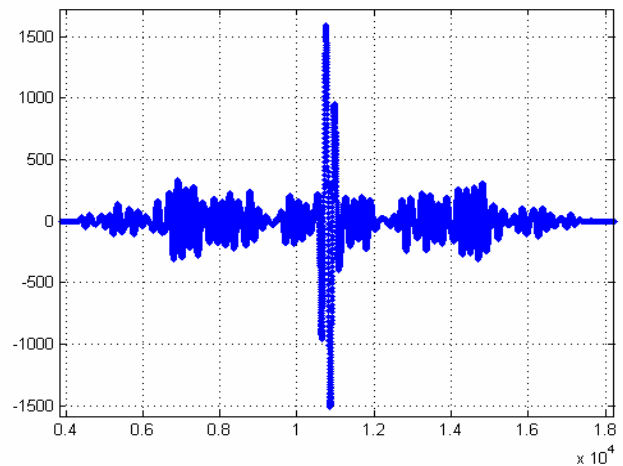


Fig.11. Experimental CCF for the binary maximum length sequence for the length of 31

In summary, using several phase manipulated pulses in the excitation packet, and subsequent coherent accumulation of the response increases the SNR in a way similar to averaging. Experimental CCFs show lowest side lobes for the Barker code of length 13 among the options considered.

VI. TESTING THE SCALABILITY OF THE PLATFORM

Scalability of the platform was tested by using two different FPGA boards. These boards contained different FPGA chips belonging to Virtex II and Spartan 3 families [17], and were connected to the host computer by different physical means - using a PCI bus and a JTAG cable respectively. The migration from one to another board was intended to reduce the cost of the FPGA chip from hundreds to tens USDs. Although the less capable chip, as one might expect, did not provide the same amount of memory to hold the data samples as the more capable one, the design was found both operational and functional in the real-time user-controlled co-simulation mode. The Spartan 3 development board [18] was complemented by a high-speed ADC board because of inadequate clock frequency of the ADC available on the Spartan board for ultrasonic instrumentation. The operation of the design was found satisfactory and met design specifications (an example of a waveform acquired is shown in fig.12).

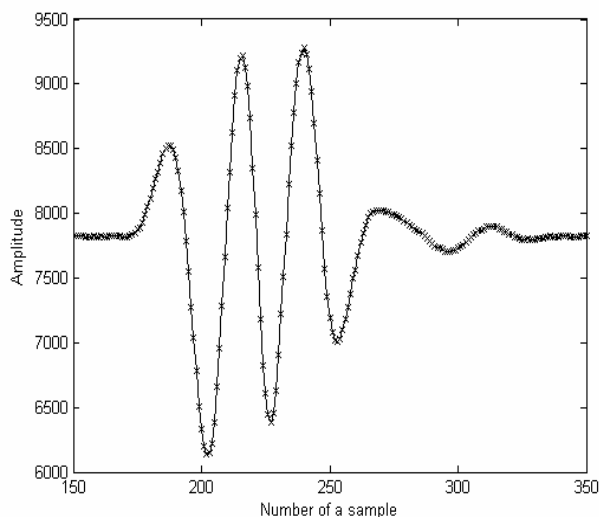


Fig.12. An example waveform acquired with a lower specification FPGA board that shows both high sampling frequency and low level of noise achieved by accurate interleaved sampling [7,8] and averaging [9]

VII. SUMMARY AND CONCLUSION

The developed research platform showed its usefulness for self-calibrating ultrasonic measurements, scalability to different hardware platforms, frame jitter free operation, utilization of coded excitation, and applicability for manual triggering. It was applied to measurements in chemical and biological reactors successfully, which confirmed its advantages as a research NDE platform.

ACKNOWLEDGEMENTS

The authors gratefully acknowledge support for this study from the UK Engineering and Physical Sciences Research Council. Chemical experiments were prepared and carried out by Dr Kirill Shafran. Dr Melissa Mather and Lisa White planned and conducted experiments in the biological reactor.

REFERENCES

- [1] G.E.Trahey, K.Ferrara, J.B.Fowlkes et al, "Ultrasonic imaging: infrastructure for improved imaging methods", Report of the OWH/NCI sponsored workshop, Mar 1999, <http://imaging.cancer.gov/reportsandpublications/ReportsandPresentations/UltrasoundImagingInfrastructureonImprovedImagingMethods>, assessed March 2007.
- [2] IEEE Transactions on Ultrasonics, Ferroelectrics and Frequency Control, vol.53, No 10, October 2006, special issue on Novel Equipment for Ultrasonic Research.
- [3] K.L.Shafran, C.C.Perry, V.Ivchenko, R.E.Challis, A.K.Holmes and A.N.Kalashnikov, "Resolving complex chemical processes: comparison of monitoring by ultrasound with other measurement methods", Proc. 2006 IEEE Instrum. Measur. Technol. Conf., pp.714-719.
- [4] ndtsolutions.com, assessed March 2007.
- [5] A.N.Kalashnikov and R.E.Challis, "Errors and uncertainties in the measurement of ultrasonic wave attenuation and phase velocity", IEEE Trans. Ultrason., Ferroel., Freq. Contr., vol.52, iss.10, Oct.2005, pp.1754 - 1768.
- [6] J.Martinsson, J.E.Carlson and J.Niemi, "Model-based phase velocity and attenuation estimation in wideband ultrasonic measurement systems", IEEE Trans. Ultrason., Ferroel., Freq. Contr., vol.54, iss.1, Jan 2007, pp.138 - 146.
- [7] V. Ivchenko, A. N. Kalashnikov, R. E. Challis, B. R. Hayes-Gill and A.K. Holmes, "Accurate Interleaved Sampling of Repetitive Ultrasonic Waveforms: Two Clock Timing Architecture and its FPGA Implementation", 2006 IEEE Instrum. Measur. Technol. Conf., Sorrento, pp.1374-1379.
- [8] V.Ivchenko, A.N.Kalashnikov, R.E.Challis, B.R.Hayes-Gill, "High-speed Digitizing of Repetitive Waveforms Using Accurate Interleaved Sampling", IEEE Trans. Instrum. Measur., accepted on 2 Feb 2007 for August 2007 issue
- [9] A.N.Kalashnikov, V.Ivchenko and R.E.Challis, "VLSI architecture for repetitive waveform measurement with zero overhead averaging" 2005 IEEE Int. Workshop Intelligent Signal Proc., 1-3 Sept. 2005, Faro, pp.334 - 339.
- [10] A.N.Kalashnikov, R.E.Challis, M.U.Unwin and A.K.Holmes, "Effects of frame jitter in data acquisition systems", IEEE Trans. Instrum. Meas., vol.54, iss.6, pp. 2177 - 2183, Dec 2005.
- [11] A. N. Kalashnikov, V. Ivchenko, R. E. Challis and B. R. Hayes-Gill, "High Accuracy Data Acquisition Architectures for Ultrasonic Imaging", accepted by IEEE Trans. Ultrason., Ferroel. Freq. Control on 20 July 2006 for publication in the special issue on High Resolution Ultrasonic Imaging in Industrial, Material and Biomedical Applications.
- [12] A.N.Kalashnikov, V.Ivchenko, R.E.Challis and A.H.Holmes, "Compensation for temperature variation in ultrasonic chemical process monitoring", 2005 IEEE Ultrasonics Symp., vol.2, 18-21 Sept 2005, Rotterdam, pp. 1151-1154.
- [13] ndtsolutions.com, accessed March 2007.
- [14] <http://en.wikipedia.org/wiki/Chirp>, accessed March 2007.
- [15] http://en.wikipedia.org/wiki/Barker_code, accessed March 2007.
- [16] <http://en.wikipedia.org/wiki/N-sequences>, accessed March 2007.
- [17] www.xilinx.com, accessed March 2007.
- [18] <http://www.nuhorizons.com/xilinx/boards/spartan-3/SP3eStarterKit/index.asp>, accessed March 2007.